Evidence for the Importance of Trapped Particle Resonances for Resistive Wall Mode Stability in High Beta Tokamak Plasmas

H. Reimerdes, J. W. Berkery, M. J. Lanctot, A. M. Garofalo, J. M. Hanson, Y. In, M. Okabayashi, S. A. Sabbagh, and E. J. Strait

Phys. Rev. Lett. **106**, 215002 — Published 23 May 2011

DOI: 10.1103/PhysRevLett.106.215002

Evidence for the importance of trapped particle resonances for resistive wall mode stability in high beta tokamak plasmas

H. Reimerdes[1,a], J.W. Berkery[1], M.J. Lanctot[1,b], A.M. Garofalo[2], J.M. Hanson[1,3], Y. In[4], M. Okabayashi[5], S.A. Sabbagh[1], and E.J. Strait[2]

[1]*Department of Applied Physics and Applied Mathematics, Columbia University, New York, NY 10027-6902, USA*

[2]*General Atomics, PO Box 85608, San Diego, California 92186-5608, USA*

[3]*Oak Ridge Institute for Science & Education, Oak Ridge, Tennessee 37831, USA*

[4]*FAR-TECH, Inc., 3550 General Atomics Ct, San Diego, California 92121, USA*

[5]*Princeton Plasma Physics Laboratory*, PO Box 451, *Princeton, New Jersey 08543-0451, USA*

Abstract. Active measurements of the plasma stability in the DIII-D tokamak reveal the importance of kinetic resonances for resistive wall mode (RWM) stability. The rotation dependence of the magnetic plasma response to externally applied quasi-static $n=1$ magnetic fields clearly shows the signatures of an interaction between the RWM and the precession and bounce motions of trapped thermal ions, as predicted by a perturbative model of plasma stability including kinetic effects. The identification of the stabilization mechanism is an essential step towards quantitative predictions for the prospects of "passive" RWM stabilization, i.e. without the use of an "active" feedback system, in fusion-alpha heated plasmas.

---

[a]Present address: CRPP-EPFL, CH-1015 Lausanne, Switzerland

[b]Present address: Lawrence Livermore National Laboratory, Livermore, CA, USA

Stable confinement of high temperature tokamak plasmas requires that the resistive wall mode (RWM) remains stable. While ideal magneto-hydrodynamic (MHD) theory predicts that the RWM becomes unstable when the normalized plasma pressure $\beta = 2\mu_0 \langle p \rangle_V / B_0^2$, where $\langle p \rangle_V$ is the volume averaged pressure and B_0 is the magnetic field on the axis, exceeds a critical value [1], early high-β experiments observed that tokamaks can operate above the ideal MHD stability limit [2]. The RWM stabilization was initially believed to require high plasma rotation [3,4], which in present day high-β tokamaks is mainly driven by the toroidal torque of tangential neutral beam injection (NBI) heating. A stabilization mechanism that relies on high plasma rotation would naturally extrapolate unfavorably to fusion-alpha heated plasmas. Fortunately, improvements in rotation control and in the correction of non-axisymmetric perturbations of the nominally axisymmetric magnetic field allowed to reduce the rotation well below the threshold previously thought to be required for RWM stability [5–7]. In this work we present compelling experimental evidence that the observed RWM stability over a wide range of plasma rotation is caused by a wave-particle interaction between the perturbed field and the motion of particles, notably the precession and bounce motion of trapped thermal ions. The measurements, in particular, demonstrate the counter-intuitive improvement of RWM stability at low rotation. The experimental results are found to be consistent with a recent low-frequency extension of kinetic theory [8].

It is well established that the interaction between non-axisymmetric perturbations and the motion of particles can have important consequences for the stability of tokamak plasmas. The energy transfer between MHD perturbations and particles can be destabilizing as in the case of “fishbones” [9], or stabilizing, as in the case of “giant” or “monster” sawteeth [10]. In both cases fast ions generated by various heating schemes interact with the MHD mode. It has been suggested that kinetic effects, of both fast and thermal particles, are also important to stabilize the RWM [11]. The RWM is a global

long-wavelength kink mode, which is only unstable when the perturbed flux can penetrate the conducting structure surrounding the plasma [1]. The low resistivity of typical vessel materials thereby limits the growth rate γ_{RWM} and toroidal rotation ω_{RWM} of the RWM to a resistive diffusion time scale of the vessel wall τ_W. According to ideal MHD theory, the RWM is unstable when the plasma exceeds the ideal MHD no-wall limit, which is the stability limit calculated for an ideal conducting plasma without any boundary constraints. The observation of stable tokamak plasmas with β above the no-wall limit [2] therefore demonstrates the importance of non-ideal modifications to RWM stability. The original kinetic stability model [11], which includes the effects of the transit motion of passing particles and the bounce motion of trapped particles, has been extended to lower frequencies by including the precession drift of trapped particles [8]. This model is successfully used to explain the observed RWM stability in low rotation DIII-D plasmas [12] and the unstable RWM onset at intermediate plasma rotation in NSTX [13].

The DIII-D tokamak [14] is well suited to study the stability of high-β plasmas. The close fitting conducting DIII-D wall, shown in Fig. 1(a), can lead to a significant gain in β through wall stabilization. The characteristic diffusion time of the wall for the $n=1$ kink mode, where n is the toroidal mode number, is approximately $\tau_W = 2.5$ ms. DIII-D routinely exceeds the ideal MHD no-wall limit and allows for sustained operation up to the ideal wall limit, which is the stability limit calculated for an ideal conducting plasma assuming an ideal conducting vessel wall [15]. Furthermore, stable operation above the no-wall limit can be achieved even at very low plasma rotation (with $\Omega\tau_A[q=2]$ as low as 0.3%), provided that the error field is sufficiently well corrected [5]. Here, the toroidal plasma rotation Ω has been evaluated at the flux surface with a safety factor $q=2$ and normalized with the inverse of the local Alfvén time defined as $\tau_A = R_0(\mu_0\rho)^{1/2}/B_0$, with R_0 being the major radius of the magnetic axis and ρ the local mass density.

Simultaneous tangential neutral beam injection (NBI) heating in the co- and counter-plasma current direction allows for independent control of the plasma pressure and the toroidal plasma rotation. Two sets of non-axisymmetric coils, including the I-coil shown in Fig. 1(a), can be used to probe the plasma stability.

Figure 1 shows an example of a low-rotation discharge in the wall-stabilized regime. The experiment is carried out using a toroidal field of $B_0 = 1.7$ T, and a plasma current of $I_P = 1.2$ MA resulting in a safety factor at the 95% flux surface of $q_{95} = 4.0$. The evolution of the normalized beta, $\beta_N = \beta[\%]/(I_P[\mathrm{MA}]/(a[\mathrm{m}]B_0[\mathrm{T}]))$, where a is the minor plasma radius, is controlled with NBI feedback. The electron density n_e, Fig. 1(c), and electron temperature T_e, Fig. 1(d), are measured by Thomson scattering and the carbon impurity density n_C, Fig. 1(c), ion temperature T_i, Fig. 1(d), and rotation Ω_C, Fig. 1(e), by charge exchange recombination spectroscopy using C VI emission. The toroidal rotation associated with the radial electric field $\omega_E \equiv -d\phi/d\psi$, with ϕ being the electrostatic potential and ψ the poloidal flux, Fig. 1(e), is derived from poloidal and toroidal rotation measurements. The fast ion density, n_{fast}, Fig. 1(c), is obtained from a Monte-Carlo calculation of the collisional slowing of fast beam ions. Quasi-neutrality then yields an estimate of the deuterium density, n_D, Fig. 1(c). Stability calculations are carried out for an equilibrium at $\beta_N \approx 2.3$ ($t = 3.0$ s), Fig. 1(e), that is reconstructed using the kinetic profiles, Fig. 1(c,d), as well as internal measurements of the current profile by a motional-Stark effect diagnostic. Ideal MHD stability calculations with the DCON code [16] yield a no-wall limit of $\beta_{N,nw} = 1.95$ and an ideal wall limit of $\beta_{N,iw} = 2.75$. The high value of β_N is maintained for many energy confinement times τ_E and several hundred characteristic wall times τ_W without an RWM becoming unstable, Fig. 1(a). A set of similar discharges with the NBI torque T_{NBI} ranging from 1.5 Nm to 8.0 Nm yields various experimentally stable ω_E rotation profiles, shown in

Fig. 2. Within this set of stable rotation profiles the normalized rotation $\omega_E \tau_A$ evaluated at the $q = 2$ surfaces varies from 0.3% to 1.5%.

The stabilization of the RWM at such low values of plasma rotation indicates the importance of particle drifts. Various particle frequencies such as a characteristic transit frequency of passing thermal ions, $\omega_t \approx V_{i,th}/(qR)$, a characteristic bounce frequency of trapped thermal ions, $\omega_b \approx [r/(2R)]^{0.5} V_{i,th}/(qR)$, and a characteristic (magnetic) precession frequency of trapped thermal ions, $\langle \omega_D \rangle_b \approx q V_{i,th}^2/(\omega_{ci} r R)$, for the investigated discharges are compared with the ω_E rotation profiles in Fig. 2. Here $V_{i,th}$ is the ion thermal velocity, R the major radius, r the minor radius, ω_{ci} the ion cyclotron frequency and $\langle\ \rangle_b$ denotes bounce averaging. Since the exact values (and signs) depend on the particle energy and pitch angle as well as details of the equilibrium, the profiles shown in Fig. 2 only indicate the order of magnitude. While the plasma rotation obtained with high NBI torque is comparable to typical bounce frequencies over a large portion of the profile, the plasma rotation obtained with the lowest values of NBI torque is of the order of the precession drift frequency. The movement of particles in the perturbed field of the RWM can modify the perturbed energy of the mode. Kinetic RWM stability models at first only took into account the transit frequency of passing particles and the bounce frequency of trapped particles [11], which typically resulted in critical rotation frequencies (normalized with the inverse Alfvén time and evaluated at the $q = 2$ surface) ranging from 0.5% to 1.0% [4,17]. Only the inclusion of the precession drift of trapped particles [8] extended the stabilization mechanism to lower rotation frequencies consistent with DIII-D balanced beam results of RWM stability down to low rotation [12]. In contrast to other instabilities the mode rotation frequency of the RWM ω_{RWM} is constrained by resistive diffusion through the wall and is therefore negligibly small. The kinetic effects are predicted to be particularly stabilizing for the RWM when a particle frequency cancels ω_E, which then leads to a resonance and dissipation. The

manifestation of these resonances in an experimental rotation scan is however not immediately evident since the overall effect on the RWM is the result of an integration over the entire particle distribution function and the plasma volume. In addition the contribution of fast ions from NBI heating, which have higher drift frequencies and primarily act as a non-dissipative restoring force independent of plasma rotation [7], can mask the resonant behavior. These experiments therefore seek to minimize the effect of NBI ions by reducing their contribution to the kinetic energy of the plasma from 35% in previous RWM experiment [5] to approximately 20% by operating at higher density and higher plasma current.

A perturbative calculation of the RWM growth rate γ_{RWM} and RWM rotation frequency ω_{RWM} based on a variational principle [18] is implemented in the MISK code [7]. The calculation of the kinetic contribution to the perturbed energy δW_K is based on the marginally unstable kink-mode structure. A systematic rotation scan, shown in Fig. 3(a), is generated by fitting a low order polynomial to the T_{NBI} dependence of the experimental rotation, Fig. 2, at each radius. The fitting procedure also allows for an extension of the experimental rotation range to lower and higher NBI torque values. The MISK code correctly predicts a negative RWM growth rate, i.e. stability, across the entire range of T_{NBI}, Fig. 3(b). The RWM is particularly stable at low plasma rotation [$\omega_E \tau_A (q=2) < 0.6\%$] and at higher rotation [$\omega_E \tau_A (q=2) > 1.4\%$]. The Alfvén time at the $q=2$ surface in these discharges is typically $\tau_A = 0.5$ μs. The stability at low rotation is attributed to an enhanced interaction of the RWM with precessing trapped thermal ions, and the stability at high rotation to an enhanced interaction with their bounce motion [13,19]. In addition to γ_{RWM}, the RWM mode rotation frequency ω_{RWM} is also predicted to have a distinct dependence on the plasma rotation, Fig. 3(c). The kinetic model in the MISK code predicts that it is important to include the stabilizing effect of the fast ions from NBI heating. Neglecting the contribution from fast ions generally leads

to an increase of the RWM growth rate, Fig. 3(b). However, the reduction is almost independent of the plasma rotation.

The predicted rotation dependence of the RWM stability manifests itself in the measured rotation dependence of the plasma response to externally applied $n=1$ fields. The set of discharges with various rotation profiles shown in Fig. 2 is probed with a low amplitude ($I_{\mathrm{I-coil}} = 350$ A) slowly rotating ($f_{\mathrm{ext}} = 20$ Hz) $n=1$ magnetic field using non-axisymmetric currents in the DIII-D I-coils. The slow toroidal rotation of the external field, which is negligible with respect to any of the plasma frequencies shown in Fig. 2, allows for coherent detection of the $n=1$ plasma response using toroidal arrays of magnetic sensors [20]. The measurements of the perturbed radial field, for example with an array of saddle loops at the outboard midplane, shown in Fig. 1(a), yield the largest amplitude of the plasma response, $\delta \mathbf{B}_{\mathrm{r}}^{\mathrm{plas}}$, when $\omega_{\mathrm{E}}\tau_{\mathrm{A}}(q=2) \approx 0.9\%$, Fig. 4(a). This plasma rotation frequency coincides with the gap between the typical precession and bounce frequencies of trapped particles. The amplitude decreases at higher as well as at lower plasma rotation. The largest phase shift of the plasma response with respect to the I-coil field at the midplane, with the plasma response trailing the I-coil by 70 degrees, is observed when $\omega_{\mathrm{E}}\tau_{\mathrm{A}}(q=2) \approx 0.6\%$, Fig. 4(b).

The amplitude and phase shift of the plasma response can be linked to the RWM growth rate and mode rotation frequency via a single-mode model [21,22]. The applicability of the single-mode model has been demonstrated in a scan of the rotation frequency of the external field ω_{ext} [20]. The model relies on an empirical coupling coefficient M_{sc}^{*}, which depends mainly on the geometry of the coil, the mode structure and the geometry of the magnetic sensors used. A scan of ω_{ext} using the I-coil in similar shaped plasmas previously yielded $M_{\mathrm{sc}}^{*} = (1.0 + 0.3i)$G/kA [20]. Using this coupling coefficient and the RWM growth rate and mode rotation frequency from the MISK predictions, Fig. 3(b,c), and comparing the resulting plasma response amplitudes and

toroidal phase shifts with the measurements yields good agreement, Fig. 4. The model reproduces in particular the largest amplification for the rotation profiles with $\omega_E \tau_A (q=2) \approx 1\%$ as well as the largest toroidal phase shift at a distinctively lower plasma rotation. Due to a large uncertainty in the coupling coefficient M_{sc}^{*} the good quantitative agreement between measurements and modeling may be partially fortuitous. Further uncertainties arise from the perturbative approach in the MISK model, from uncertainties in the fast ion content and from the simplified assumption being used for the fast ion distribution function in the MISK code [7]. The main result is the reproduction of the qualitative characteristics of the plasma rotation dependence of the plasma response by the kinetic stability model. The features at low rotation are directly related to the resonance with the precession frequency of the trapped (thermal) ions, revealing that the predicted effects [8,11] are indeed relevant for RWM stability.

In conclusion, measurements of the rotation dependence of the amplitude and phase of the plasma response to externally applied $n=1$ fields in DIII-D reveal the features of the interaction of the stable RWM with the precession and bounce motion of trapped thermal ions and thereby yield evidence for the importance of these kinetic effects for the stability of high β plasmas. An important feature of the resonance of the RWM with precessing trapped thermal ions is improved stability at very low plasma rotation. This improved stability supports the hypothesis [23] that it is not the onset of an RWM, which leads to the previously reported rotation threshold of $\Omega\tau_A (q=2) \approx 0.3\%$ in high β DIII-D discharges [5]. More importantly, it has the potential to allow for "passive" RWM stabilization in advanced reactor scenarios. The present DIII-D results identify the relevance of kinetic effects, but in order to gain confidence in any extrapolation of the potential of passive RWM stabilization from today's NBI heating dominated experiments to a burning plasma (e.g. [7,8,24]), the qualitative understanding must evolve into quantitative predictions.

This work was supported in part by the US Department of Energy under DE-FG02-89ER53297, DE-FG02-06ER84442, DE-FC02-04ER54698, and DE-AC02-09CH11466. The authors would like to thank Drs. M.S. Chu, J.P. Graves and Y. Liu for enlightening discussions.

[1] J.P. Freidberg, *Ideal Magnetohydrodynamics* (Plenum Press, New York, 1987).

[2] E.J. Strait, *et al.,* Phys. Rev. Lett. **74**, 2483 (1995).

[3] A.M. Garofalo, *et al.*, Phys. Rev. Lett. **82**, 3811 (1999).

[4] R.J. La Haye, *et al*., Nucl. Fusion **44**, 1197 (2004).

[5] H. Reimerdes, *et al.,* Phys. Rev. Lett. **98**, 055001 (2007).

[6] M. Takechi, *et al.,* Phys. Rev. Lett. **98**, 055002 (2007).

[7] J.W. Berkery, *et al*., Phys. Plasmas **17**, 082504 (2010).

[8] B. Hu and R. Betti, Phys. Rev. Lett. **93**, 105002 (2004).

[9] K. McGuire *et al*., Phys. Rev. Lett. **50**, 891 (1983).

[10] F. Porcelli, Plasma Phys. Control. Fusion **33**, 1601 (1991).

[11] A. Bondeson and M.S. Chu, Phys. Plasmas **3**, 3013 (1996).

[12] H. Reimerdes *et al*., Plasma Phys. Control. Fusion **49**, B349 (2007).

[13] J.W. Berkery *et al*., Phys. Rev. Lett. **104**, 035003 (2010).

[14] J.L. Luxon, Nucl. Fusion **42**, 614 (2002).

[15] A.M. Garofalo *et al.*, Phys. Rev. Lett. **89**, 235001 (2002).

[16] A. Glasser and M.S. Chance, Bull. Am. Phys. Soc. **49**, 1848 (1997).

[17] H. Reimerdes *et al.*, Phys. Plasmas **13**, 056107 (2006).

[18] S.W. Haney and J.P. Freidberg, Phys. Fluids B **1**, 1637 (1989).

[19] I.T. Chapman *et al*., Plasma Phys. Control. Fusion **51**, 055015 (2009).

[20] H. Reimerdes *et al*., Phys. Rev. Lett. **93**, 135002 (2004).

[21] M.S. Chu *et al*., Nucl. Fusion **43**, 196 (2003).

[22] V.D. Pustovitov, Plasma Phys. Rep. **30**, 187 (2004).

[23] H. Reimerdes, *et al.,* Bull. Am. Phys. Soc. **53**, PO3.00011 (2008).

[24] Y.Q. Liu, Nucl. Fusion **50**, 095008 (2010).

LIST OF FIGURE CAPTIONS

FIG. 1. (a) Poloidal cross section of the DIII-D vessel and a typical equilibrium used in this study. (b) The time evolution of β_N indicates sustained stable operation above the calculated ideal MHD no-wall limit. Measured density (c), temperature (d) and rotation profiles (e) as a function of the square root of the normalized poloidal flux ρ_p.

FIG. 2. A shot-to-shot scan of the NBI torque T_{NBI} at constant β_N yields a wide range of stable ω_E rotation profiles (solid), which are compared with typical transit ω_t (dotted), bounce ω_b (dashed) and magnetic precession drift $\langle\omega_D\rangle$ (dash-dotted) frequencies of thermal ions. The radial coordinate is the square root of the normalized toroidal flux ρ_t.

FIG. 3. (a) Smoothed stable ω_E rotation profiles as a function of the square root of the normalized toroidal flux ρ_t and kinetic calculations of (b) the RWM growth rate and (c) RWM rotation frequency using the MISK code as a function of ω_E at $q = 2$ normalized with the inverse of the Alfvén time τ_A.

FIG 4. Comparison of the measured (squares) and modeled (line) rotation dependence of the (a) amplitude and (b) toroidal phase shift of the plasma response to a slowly rotating (f_{ext} = 20 Hz) externally applied $n = 1$ field. The plasma response $\delta\mathbf{B}_{r,l}^{plas}$ is measured with radial field sensors, the external field applied with the I-coil and the ω_E rotation normalized with τ_A^{-1} and evaluated at $q \approx 2$.

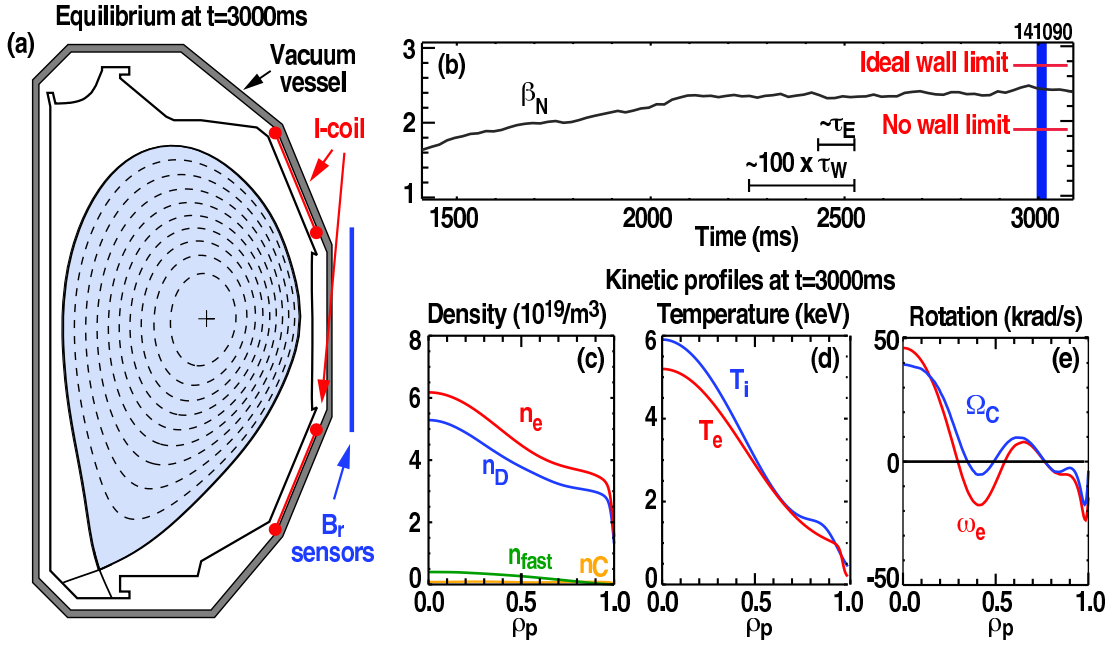

H. Reimerdes Figure 1

Figure 1 LZ12548 11FEB2011

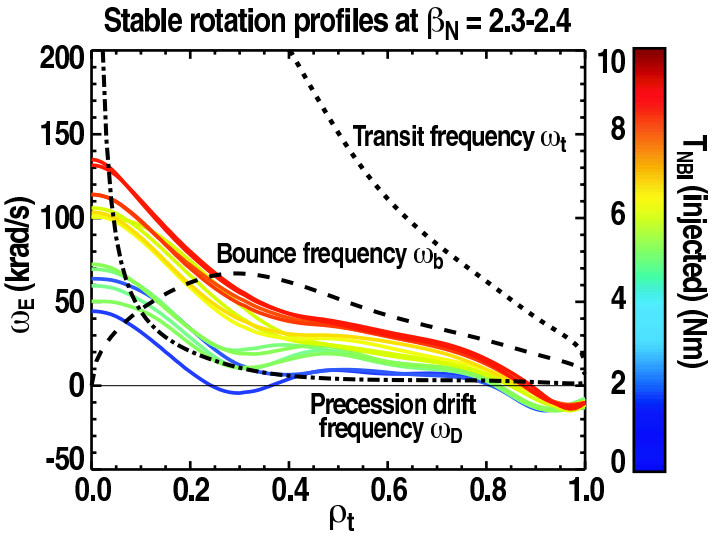

H. Reimerdes Figure 2

Figure 2 LZ12548 11FEB2011

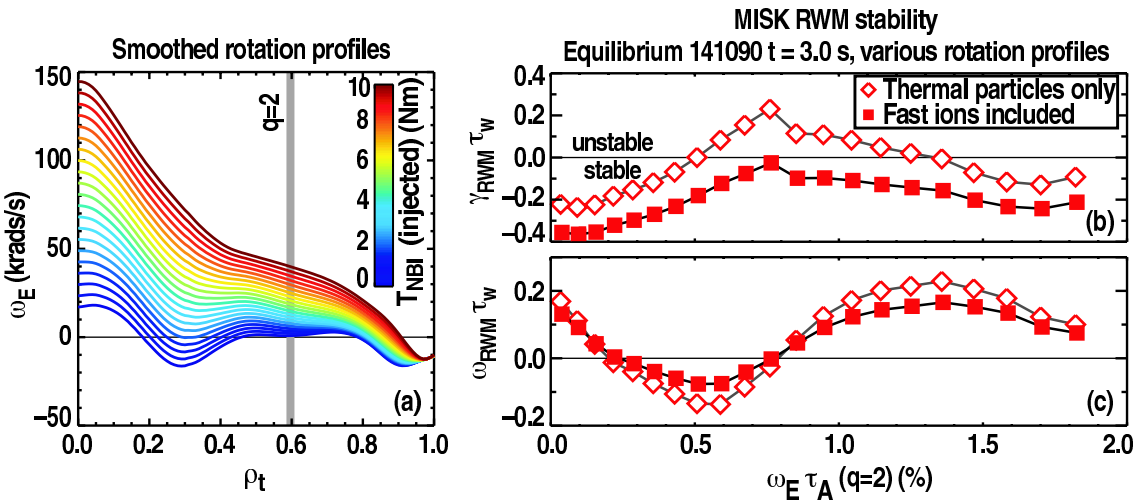

H. Reimerdes Figure 3

Figure 3 LZ12548 11FEB2011

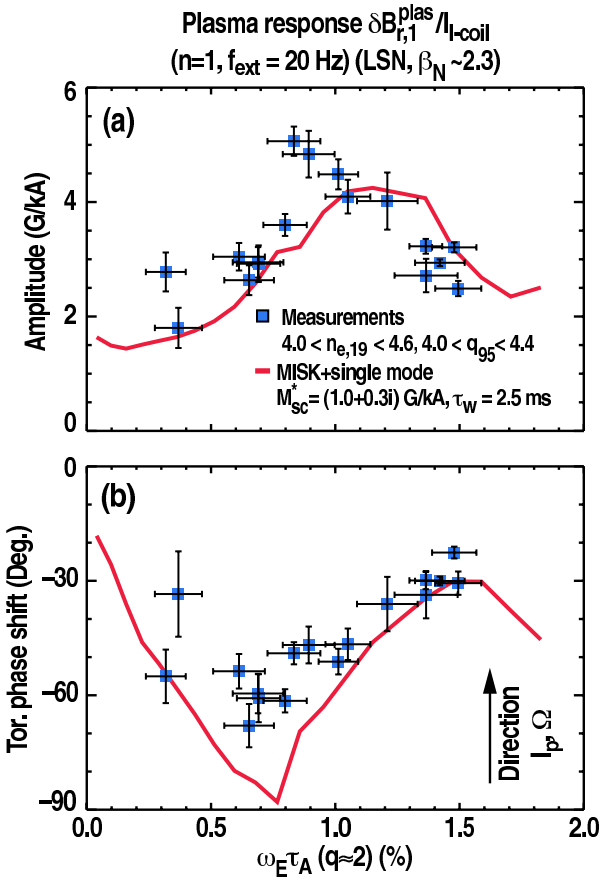

H. Reimerdes Figure 4

Figure 4 LZ12548 11FEB2011